Title
ACTINIDE-SPECIFIC COMPLEXING AGENTS: THEIR STRUCTURAL AND SOLUTION CHEMISTRY

Authors
Raymond, K.N.
Freeman, G.E.
Kappel, M.J.

Publication Date
1983-07-01

Lawrence Berkeley Laboratory

UNIVERSITY OF CALIFORNIA

Materials & Molecular Research Division

To be presented at the First International Conference on the Chemistry and Technology of the Lanthanides and Actinides, Venice, Italy, September 5-10, 1983

ACTINIDE-SPECIFIC COMPLEXING AGENTS: THEIR STRUCTURAL AND SOLUTION CHEMISTRY

K.N. Raymond, G.E. Freeman, and M.J. Kappel

July 1983

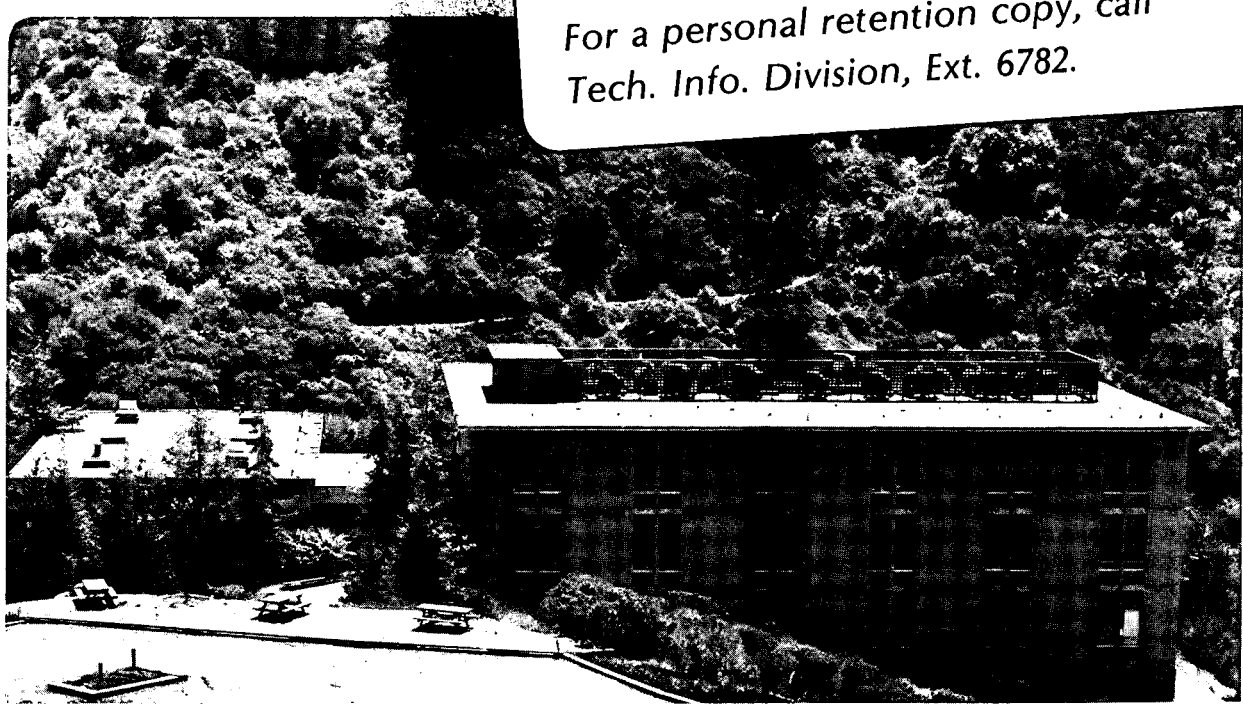

Prepared for the U.S. Department of Energy under Contract DE-AC03-76SF00098

DISCLAIMER

Actinide-Specific Complexing Agents: Their Structural and Solution Chemistry

by

Kenneth N. Raymond, Gwen E. Freeman, and Mary J. Kappel

Department of Chemistry and Materials and Molecular Research Division,

Lawrence Berkeley Laboratory, University of California,

Berkeley, California 94720

This work was supported by the Director, Office of Energy Research, Office of Basic Energy Sciences, Chemical Sciences Division of the U.S. Department of Energy under Contract Number DE-AC03-76SF00098

Introduction

With the commercial development of nuclear reactors, the actinides have become important industrial elements. A major concern of the nuclear industry is the biological hazard associated with nuclear fuels and their wastes.[1,2] In addition to their chemical toxicity, the high specific activity of alpha emission exhibited by the common isotopes of the transuranium elements make these elements potent carcinogens when incorporated.[3-7] Since biological systems are unable to detoxify metal ions by metabolic degradation, they instead must be excreted or immobilized.[8] Unfortunately, only a small portion of absorbed tetra- or trivalent actinide is eliminated from a mammalian body during its lifetime. The remaining actinide is distributed throughout the body but is especially found fixed in the liver and in the skeleton.[5,7,9-12] While the ability of some metals to do damage is greatly reduced by immobilization, local high concentrations of radioactivity are produced by immobilized actinides — thereby increasing the absorbed radiation dose and carcinogenic potential. Removal of actinides from the body is therefore an essential component of treatment for actinide contamination.

Conventional chelating agents such as diethylenetriaminepentaacetic acid, DTPA, remove much of the soluble actinide present in body fluids, but are almost totally ineffective in removing the actinide after it has left the circulation or after hydrolysis of the metal to form colloids and polymers.[13-15] The inability of DTPA to completely coordinate the tetravalent actinides is shown by the easy formation of ternary complexes between Th(DTPA) and many bidentate ligands.[16-18] The hydrolysis of Th(IV) and U(IV) DTPA complexes at pH near 8 is explained by the

dissociation of H^+ from a coordinated water molecule.[19-22] In addition, the polyaminocarboxylic acids are relatively toxic because they indiscriminately complex and remove biologically important metals, especially zinc.[23-26] Thus there is a need to develop new and powerful chelating agents highly specific for tetravalent actinides, particularly Pu(IV).

While not the most toxic, plutonium is the most likely transuranium element to be encountered. Plutonium commonly exists in aqueous solution in each of the oxidation states from III to VI. However, under biological conditions redox potentials, complexation, and hydrolysis strongly favor Pu(IV) as the dominant species.[27,28] For this reason, the early work of our research group focused on developing sequestering agents specific for Pu(IV) and the other tetravalent actinide ions.

There are remarkable similarities between Pu(IV) and Fe(III) (Figure 1). These include the similar charge per ionic radius ratios for Fe(III) and Pu(IV) (4.6 and 4.2 e/Å, respectively), and the formation of highly insoluble hydroxides. They also have similar transport properties in mammals; the majority of soluble Pu(IV) present in body fluids is rapidly bound by the iron transport protein transferrin at the site which normally binds Fe(III). In liver cells, deposited plutonium is initially bound to the iron storage protein ferritin and eventually becomes associated with hemosiderin and other long-term iron storage proteins.[9,29,30] These similarities of Pu(IV) and Fe(III) suggested to us a biomimetic approach to the design of Pu(IV) sequestering agents modeled after the very efficient and highly specific iron sequestering agents, siderophores, which are used by bacteria and other microorganisms to obtain Fe(III) from the environment.[31-33]

The siderophores (Figure 2) typically contain hydroxamate or catecholate functional groups which are arranged to form an octahedral cavity the exact size of a ferric ion. Catechol (2,3-dihydroxybenzene) and the hydroxamic acids (N-hydroxyamides) are very weak acids that ionize to form "hard" oxygen anions, which bind strongly to strong Lewis acids such as Fe(III) and Pu(IV). Complexation by these groups forms five-membered chelate rings, which substantially increases their stability compared to complexation by lone oxygen anions.[34] Due to its higher charge and strong basicity, the catecholate group forms even stronger complexes with the tetravalent actinides than the hydroxamate anion. Thus our initial goal was the incorporation of catecholate functional groups into multidentate chelating agents that specifically encapsulate tetravalent actinides. This has led to the examination of the solution chemistry of Pu(III) and (IV) with catechol and catecholate ligands.

In addition, we have recently examined the relatively unknown catecholate coordination chemistry of the trivalent actinide ions in order to understand the unusual excretion behavior of americium(III) observed in mice and dogs treated with catecholate ligands we have developed.[35,36] It was initially thought that this behavior resulted from the tetracatechoylamide ligands stabilizing the americium(IV) oxidation state, but we have recently shown[36] that americium exists in the trivalent state in catecholate complexes. Although the early transuranium actinides exhibit a wide variety of oxidation states, in their trivalent state they have ionic radii and chemical properties similar to the trivalent lanthanides in the same column of the periodic

table.[37] Since the stability and coordination chemistry of metal catecholate complexes are largely determined by the metal's charge to ionic radius ratio[38,39] we have begun to explore the lanthanide(III) catecholates as models for actinide(III) catecholate complexes.[40,41]

The similarity between Fe(III) and actinide(IV) ions ends with their coordination numbers. Because of the larger ionic radii of the actinide(IV) ions, their preferred coordination number is eight or more (higher coordination numbers usually occur with very small ligands or by the incorporation of a solvent molecule[42,43]). The two stable high-symmetry eight-coordinate geometries are the square antiprism (D_{4d}) and the trigonal faced dodecahedron (D_{2d}). The coulombic energy differences between these polyhedra (Figure 3) is very small and the preferred geometry is largely determined by steric requirements and ligand field effects. Cubic coordination lies at higher energy because of higher ligand-ligand interactions and thus is seen only in the solid state. Another important eight-coordinate polyhedron, the bicapped trigonal prism (C_{2v}), corresponds to an energy minimum along the transformation pathway between the square antiprism and the dodecahedron.[44-49] The mmmm isomer of the trigonal faced dodecahedron is the most prevalent polyhedron in the solid state.

Actinide Catecholates

Two fundamental questions in the design of an actinide-specific sequestering agent are the coordination number and geometry actually preferred by the metal ion with a given ligand. The complexes formed by Th(IV) or U(IV) and catechol, in which the steric restraints of a macrochelate are absent, serve as structural archetypes for designing

the optimum actinide(IV) sequestering agent. Thus the structures of an isoelectronic, isomorphous series of tetrakis-catecholato salts, $Na_4[M(C_6H_4O_2)_4]\cdot 21H_2O$; M = Th(IV), U(IV), Ce(IV), and Hf(IV), were determined by single crystal X-ray diffraction. Suitable crystals were isolated from the reaction of the metal chlorides or nitrates and the disodium salt of catechol in aqueous solution under an inert atmosphere.[50,51] Measurement of magnetic susceptibility and electronic spectra of the cerium and uranium complexes verified the presence of the +4 oxidation state.

It was somewhat surprising that the strongly oxidizing Ce(IV) ion (E_o = + 1.70 V)[52] did not react with the catechol dianion, a facile reducing agent.[53] The ability of catechol to coordinate, without reduction, oxidizing ions as Ce(IV), Fe(III),[54] V(V),[55] and Mn(IIL)[56] is a reflection of this ligand's impressive coordinating ability. The Ce(IV) complex was found by differential pulse voltammetry to undergo a quasi-reversible one-electron reduction in strongly basic solution in the presence of excess catechol. The measured potential of this was - 488 mV vs NHE. This enormous shift of the redox potential of the Ce(IV)/Ce(III) couple is dramatic evidence of the enormous affinity of the catecholate anion for the tetravalent lanthanides and actinides.[57] More details of this system and the Pu(IV)/Pu(III) couple will be given later.

The crystal structure of this isostructural series of catechol complexes consists of discrete $[M(catechol)_4]^{4-}$ dodecahedra, a hydrogen bonded network of 21 waters of crystallization and sodium ions, each of

which is bonded to two catecholate oxygens and four water oxygens. Of the possible eight coordinate polyhedra, only the cube and the dodecahedron allow the presence of the crystallographic $\bar{4}$ axis on which the metal ion sits. As depicted in Figure 4 the tetrakis(catecholato) complexes nearly display the ideal D_{2d} molecular symmetry of the mmmm-isomer of the trigonal-faced dodecahedron.

Actinide Sequestering Agents

With the geometric considerations just described in mind, four 2,3-dihydroxybenzoic acid groups were attached to a series of linear tetraamines via amide linkages as shown schematically in Figure 5. Cyclic tetramine backbones were also used. However the greater stereochemical freedom effected by linear tetraamine backbones yielded chelates significantly more effective in removing Pu(IV) from mice.[58]

The introduction of anionic electron-withdrawing substituents in the 2,3-dihydroxybenzoyl group of the ligand (Figure 6) improves their water solubility, stability to air oxidation, and affinity for the actinide(IV) ion at low pH. This initially was achieved by sulfonation in the 5-position but has also been done by introducing a carboxylate group in the 4-position (Figure 6),[59] the latter also provides another potential ligating group.

Gadolinium is located in the lanthanide series one column to the right of europium, the homolog of americium. The structural chemistry of gadolinium(III) with catechol was examined[40] to compare its unconstrained coordination geometry with that of the tetravalent actinides and lanthanides. The structure of a tetrakiscatecholato salt, $Na_5[Gd(cat)_4]\cdot 19.2H_2O$ was determined by single crystal X-ray diffraction and proved

to be nearly isomorphous with the tetrakis catecholate complexes with the tetravalent actinides discussed previously. The gadolinium tetracatecholate complex consists of discrete $[Gd(catechol)_4]^{5-}$ dodecahedra (as depicted in Figure 4), a hydrogen-bonded network of 19.2 waters of crystallization and sodium ions. Each of four of the sodium ions are bonded to two catecholate oxygens and four water oxygens, as with the M(IV) structures; the fifth sodium atom is disordered and prevents some of the waters from having a full occupancy, which results in the fractional value of 19.2 waters.

Crystals of $[Gd(catechol)_4]^{5-}$ were isolated from the reaction of the metal nitrate and a 50% excess of the disodium salt of catechol in aqueous, approximately 2 M catecholate solution under an inert atmosphere.[40] Such forcing conditions of high pH and excess catechol were necessary to obtain the tetrakis catecholate complex.

If a smaller ratio of catechol to metal is used (e.g., three or four to one) the dimeric complex $Na_6[Gd(catechol)_3]_2 \cdot 20H_2O$ is obtained. The structure of this complex was determined by single crystal X-ray diffraction. It consists of discrete units of $[Gd(cat)_3]_2^{6-}$ dimers (Figure 7). The sodium atoms and twenty waters of crystallization are in infinite bridging chains involving some of the catecholate oxygens. This bonding network greatly increases the compound's resistance to air oxidation in the solid state. Each gadolinium atom is seven coordinate and the dimer has two bridging catecholates.

The chemistry of the isolated Gd(III) complexes parallels aspects of the catechol solution chemistry of cerium and plutonium as seen electrochemically. Previous work[51,60,61] demonstrated that catechols are very good at stabilizing higher oxidation states of metal ions. In

fact, the potentials of the uncomplexed ions, normally obtained in non-coordinating acidic media, are known to shift negative in excess of 2.0 volts upon complexation of catechol in basic solution. This brings the Ce and Pu (IV)/(III) reduction potential well within the operating range of a hanging mercury drop electrode in base.[62]

By varying ligand concentrations and pH of Ce- and Pu-catecholate solutions, electrochemistry can be used to elucidate not only the relative stability of M(IV) versus M(III) complexes, but also to study the protonation behavior and stoichiometry of complexes.[63] Utilizing differential pulse voltammetry,[64] these studies can be carried out in dilute solution (less than 0.2 mM in Pu).

M(IV)/(III) Catechol Electrochemistry

The low acidity of catechol requires that the electrochemical experiments be conducted under very basic conditions. The measurements of electrochemical potential as a function of ligand concentration were always maintained at pH values > 12.3. Above this pH the potential is independent of pH and demonstrates only a ligand dependence. A large negative shift in potential for increasing total catechol concentrations is observed for Pu-catechol as compared to Pu(IV)/Pu(III) (+ 0.98 V vs NHE) in acidic medium.[65] This indicates a stabilization of the tetravalent ion relative to the trivalent ion by catechol. Similar stabilization of the Ce(IV)/Ce(III) couple with catechol is observed.[51] In addition, a similar negative shift in potential with increasing total ligand concentration is seen. Both systems are classified as quasi-reversible, since there is a dependence of peak potential on scan rate. However at the slow scan rates employed here the electrode kinetics are reversible.

If the composition of the oxidized metal complex is known, the variation of potential of an electroactive metal complex with increasing ligand concentration gives information on the stoichiometry of the reduced metal complex which is formed.[63] For plutonium, using the two half reactions (L^{2-} = catechol^{2-})

$$Pu(IV) + e^- = Pu(III) \qquad E_o = + 0.98 \text{ V vs. NHE}$$

$$Pu(IV)L_4^{4-} + e^- = Pu(III)L_q^{3-2q} + (4-q)L^{2-} \qquad E_f$$

and the two dissociation constants

$$K_{IV} = \frac{[Pu(IV)][L^{2-}]^4}{[Pu(IV)L_4^{4-}]} \qquad K_{III} = \frac{[P(III)][L^{2-}]^q}{[Pu(III)L_q^{3-2q}]}$$

A Nernstian expression can be written which includes a dependence on total ligand concentration (L_T) assuming reversible electrode kinetics at 25°C

$$E_o - E_f = 0.059 \left[\log \left(\frac{K_{IV}}{K_{III}} \right) - (4-q) \log L_T \right]$$

Differentiation of this equation gives

$$d(E_f)/d(\log L_T) = - 0.059 (4-q)$$

Thus, a plot of potential versus the log of the total ligand concentration gives a line with a slope containing the value of 4-q, where q is the stoichiometric coefficient for M(III) catechol complexes. If the stoichiometry of the M(III) catechol complex is the same as that for the M(IV) catechol complex, there would be no variation of E_f with total ligand concentration and the total potential shift would be proportional

to log (K_{IV}/K_{III}). Such a plot for cerium catechol is illustrated by Figure 8. The slope of this line indicates q = 2.5. This implies a M(III) catechol complex of lower stoichiometry than the M(IV) catechol complex with two alternate interpretations: either under the conditions specified the M(III) complex may involve 2.5 catechols or at this pH there exists an equilibrium between the biscatecholate and triscatecholate complex. These results alter earlier interpretations regarding cerium catechol electrochemistry.[51] This previous study did not include an investigation of the ligand dependence of the potential, but rather measured a potential in 5 M NaOH and 1 M catechol assuming the Ce(III) complex was a tetracatechol complex. The value reported (- 692 mV vs SCE) is included as a point in Figure 8, indicating that the same ligand dependence on the potential exists at these extreme conditions. However, there appears to be no shift in potential above catechol concentrations of 2 M (5 M KOH) which means that under these forcing conditions a tetrakis(catecholato) complex of Ce(III) predominates in solution. The reduction potential for the Ce(IV)/Ce(III)-(catechol) couple is - 732 mV vs SCE and implies a ratio of K(IV)/K(III) of 10^{41}.

The plot of potential versus the log of the total ligand concentration for plutonium-catechol (Figure 9) is very similar to that observed for cerium-catechol. The slope of that line again indicates that q = 2.5. Although the electrochemistry of these systems show quasi-reversible behavior, theory developed for reversible systems[63] appears to apply.

Although a great deal of effort has been expanded to synthesize catecholate ligands which are octadentate(tetracatecholates) and capable of encapsulating actinide(IV) ions,[59,66,67] previously there has been

no direct evidence about the nature of complexes formed — aside from the fact that 3,4,3-LICAMS and 3,4,3-LICAMC (Figure 6) effectively complex Pu(IV) *in vivo* and promote excretion.[58,59] The results of the first *in vitro* experiments of plutonium with catecholate ligands have recently been obtained.

Upon addition of Pu(IV) to a solution of 3,4,3-LICAMS at high pH (> 12) a fairly intense amber color is observed due to a broad charge transfer band at 435 nm (ε = 750 M^{-1} cm^{-1}). This same color is observed for Pu(IV) catechol at high pH. Lowering the pH of the Pu(IV)-3,4,3-LICAMS (pH 10.9) shifts λ_{max} to 441 nm (ε = 460 M^{-1} cm^{-1}), similar to the shifts and intensity loss seen for Fe(III)-3,4-LICAMS upon protonation.[68] Complexes of $Ce(IV)(cat)_4^{4-}$ are purple,[51] as is the Ce(IV)-3,4,3-LICAMS complex at high pH (λ_{max} = 514 nm, ε = 4400 M^{-1} cm^{-1}). Thus at high pH (> 12) the 3,4,3-LICAMS complexs of Pu(IV) and Ce(IV) seem to be tetracatecholate complexes.

The negative shifts in potential for the Pu(IV)- and Ce(IV)-3,4,3-LICAMS complexes as compared to free M(IV)/(III) are given in Figure 10. The shifts are larger than those observed with catechol. The potential of the Pu(IV)/(III)- and Ce(IV)/(III)-3,4,3-LICAMS couple does *not* appear to shift with increasing ligand concentration. This could mean all four catecholate groups are bound. However if upon reduction of the metal center to M(III) the number of catecholate groups bound decreases (as in the Pu and Ce catechol studies), this change would not be reflected in a change of potential with varying total ligand concentration. A shift in potential dependent on total ligand concentration will occur only if stoichiometries other than 1:1 occur.

If the Pu(III)-3,4,3-LICAMS complex is similar to the Pu(III) catechol complex, at high pH there are one or possibly two pendant arms of the macrochelate which are unbound and deprotonated. Figure 11 shows the differential pulse voltammograms of Pu(IV)-3,4,3-LICAMS as a function of pH. A positive shift in potential and a loss of current is seen between pH 10.8 and pH 6.5, whereas a small shift in potential and a small loss of current is observed between pH 12.1 and pH 11.0. Precipitation is evident at pH 9.4 and increases as the pH is lowered. This dependence of potential on pH can be due to either the acidity of the oxidized complex (and $E_{1/2}$ is only independent of pH in regions of low pH) or the acidity of the reduced complex (and $E_{1/2}$ is only independent of pH in regions of high pH).[36] A plot of $E_{1/2}$ versus pH for Pu(3,4,3-LICAMS) is shown in Figure 12. It shows a region at high pH with very little change in $E_{1/2}$ and a region between pH 10.8 and 6.5 with a slope of - 0.053. This corresponds to a one proton equilibrium[36] involving the acidity of the reduced species. The intersection of the two lines is at pH = pK_a = 11.0. If the Pu(III)-3,4,3-LICAMS has one or two pendant catechol arms free, this pK_a corresponds very well with the protonation of a phenolic oxygen meta to the carbonyl. In the free ligand, with no metal bound, this pK_a is estimated to be about 11.5.[69] Very similar results are observed for Pu(3,4,3-LICAMC) but with one notable difference, the phenolic oxygens of 3,4,3-LICAMC are considerably less acidic than those of the sulfonated ligand.[70] Thus, the protonation constants of the complexes are considerably higher.

The decrease in peak current with decreasing pH observed in Figure 11 can also be attributed to a protonation phenomenon, but the protonation here involves the Pu(IV)-3,4,3-LICAMS complex. The bulk solution

contains the Pu(IV) complex and the peak current is directly proportional to the concentration. For differential pulse at a stationary electrode the peak current can be expressed as [71]

$$\Delta i_p = \frac{nFAD^{1/2}c}{\pi^{1/2}t^{1/2}} \cdot \frac{1 - \beta}{1 + \beta}$$

where

n = number of electrons

F = Faraday constant

A = electrode area

D = diffusion coefficient of bulk electroactive species

C = concentration of bulk electroactive species

t = pulse width

$\beta = \exp[nF/RT\Delta E]$; ΔE = pulse height

Thus, one can consider that for two electroactive species in solution with differing diffusion coefficients the peak current is

$$\Delta i_p = kD_1^{1/2}c_1 + kD_2^{1/2}c_2$$

where k is a constant containing the aforementioned parameters. Consider that c_1 and c_2 be related by a protonation equilibrium

$$K_H = \frac{c_1[H^+]^n}{c_2}$$

and that $c_T = c_1 + c_2$. For this relationship an expression can be developed

$$\Delta i_p = kD_2^{1/2}c_T + \frac{(\Delta i_p^\circ - \Delta i_p)KH}{[H^+]^n}$$

where

Δi_p° = the peak current at high pH with only species c_1 present

Δi_p = the peak current at any pH other than i_p° where c_1 and c_2 are in equilibrium

This is analogous to an expression developed by Schwarzenbach for VIS-UV spectra, only in this case diffusion coefficients rather than extinction coefficients are used.[72]

A plot of Δi_p versus $(\Delta i_p^\circ - \Delta i_p)/[H^+]^n$ with proper choice of n gives a straight line with slope K_H. Figure 13 illustrates such a plot for Pu(IV)-3,4,3-LICAMS. Two straight line segments are observed. The line segment with shallow slope corresponds to the protonation:

$$Pu(IV)\text{-}3,4,3\text{-}LICAMS^{8-} + H^+ = Pu(IV)\text{-}3,4,3\text{-}HLICAMS^{7-}$$

The shift in λ_{max} in the visible spectra obtained over this pH range also indicate that protonation is occurring. The plot shown in Figure 13 implies that the monoprotonated Pu(IV) complex has a diffusion coefficient 30 - 40% smaller than that of the deprotonated Pu(IV) complex. This seems unlikely, since to a first approximation the diffusion coefficient is proportional to the volume of the complex. Therefore large changes in the diffusion coefficient would not be expected upon a single protonation. Lowering the pH further, a white flaky precipitate is formed [$Pu(OH)_4$ is green and gelatinous] and a linear decrease in current is also observed and included in Figure 13 for interest. This line segment cannot be interpreted by the same method used for the line segment of shallow slope since two species are not in equilibrium in solution as is required to use this method. Instead,

an alternate graphical method can be used. The formation constant for such a precipitate would be

$$K = \frac{1}{[Pu(IV)HLICAMS][H^+]^n}$$

Therefore, a plot of $\ell n\ \Delta i_p$ vs $\ell n\ [H^+]$ should give a line of slope = n. Such a plot for Pu(IV)-3,4,3-HLICAMS is linear (correlation = - 0.9999), but the slope is nonintegral (slope = - 0.20). Since this gives the change in the average number of bound protons on going from the oxidized to the reduced species, it may indicate a mixture of protonated species exist in this pH range. It does appear that this precipitate is at least a diprotonated Pu(IV) complex. Complexes of Pu(IV) are prone to hydrolysis and polymerization. In addition, the bridging capabilities of catechol are well illustrated in the $[Gd(III)(cat)_3]_2^{6-}$ structure, which contains two bridging catechol dianions.[40] In contrast to Pu(3,4,3-LICAMS), the Ce(3,4,3-LICAMS) differential pulse voltammogram shows no positive shift in potential with decreasing pH; however, it does show a decrease in peak current. This may reflect differences in the protonation reactions in this pH range. A summary of the protonation behavior of complexes of Pu(IV)- and Pu(III)-3,4,3-LICAMS and 3,4,3-LICAMC as determined by electrochemical methods is diagrammed in Figure 14.

The implications of this study are that the complex of Pu(IV)-3,4,3-LICAMS which exists at pH 7.4 (human plasma pH) is <u>not</u> a tetracatecholate complex. It may be a triscatecholate complex. <u>In vivo</u> studies of Pu(IV) removal from mice using the same concentrations of 3,4,3-LICAMS and 3,4-LICAMS indicate that 3,4-LICAMS is more effective <u>per functional catechol group</u>. Thus Pu(IV) does not appear to utilize the full denticity

of the tetracatechol, 3,4,3-LICAMS. Indeed, results obtained here indicate that use of functional groups more acidic than catechol may be warranted. Development of macrochelates of the more acidic N-hydroxypyridinone ligand is currently underway.

The examination of the *in vitro* complexation behavior of Pu(III) and Pu(IV) by catecholate ligands was prompted by test results which indicated that synthetic catechoylamide ligands were effective *in vivo* sequestering agents for Pu(IV).[58,59] Likewise, the study of americium-catecholate complexation was prompted by the puzzling results of *in vivo* experiments in mice and dogs on americium removal by 3,4,3-LICAMS and 3,4,3-LICAMC (*vide infra*).[35] The specificity of 3,4,3-LICAMS for metal ions of high charge to ionic radius ratios has been demonstrated by thermodynamic measurements.[73] Most biologically significant metal ion are divalent ions and this study did not investigate the stability of catecholates with trivalent ions that have smaller charge to ionic radius ratios than Fe(III). Therefore, a study of lanthanide(III) catecholate complexes in solution was begun and continues.[41] The trivalent lanthanides have been used extensively as models for trivalent actinides, since size variations between homologs of the two rows are small.[37] In particular, studies with catecholate ligands have concentrated on complexation by Eu(III), the homolog of Am(III).

Originally it was thought that complexation of Am(III) *in vivo* by catecholate ligands would not be of sufficient stability to remove Am(III) from test animals. Surprisingly, dogs injected with Am(III), followed 30 minutes later by injections of 3,4,3-LICAMS or 3,4,3-LICAMC, excreted 34% and 27%, respectively, of the Am after seven days. (Controls excreted 11%.)[35] The calcium, trisodium salt of diethylenetriamine pentaacetic

acid ($CaNa_3DTPA$) (the current therapeutic chelating agent for Am) is much more efficient at sequestering Am under similar conditions (83% excreted).

The plasma clearance curves for americium-treated dogs following injection of the catecholate ligand are particularly unusual (Figure 15).[35] These curves indicate that for the dogs injected with the catechol ligand the amount of Am in the plasma is increased and retained. Also, the slope of the lines following injection of LICAMS or LICAMC were similar to the slope of plasma clearance curves for untreated dogs injected with Pu(IV). The conclusion reached was that the injected catecholate induced the americium to circulate as a very stable transferrin complex, just as Pu(IV) circulates. Such protein complexes are not filtered out of the plasma. Although Am(III) is known to form complexes with transferrin, they are of limited stability, just as for the lanthanide(III) ions[5,74] discussed below. (See the decrease in concentration for the "untreated" clearance curve.) The increase of Am in the plasma following injection of catecholate ligand can be then attributed to the dynamic equilibrium that exists between extracellular fluid and the circulation, i.e., the Am can get in the plasma, but once in, it forms a very stable complex with transferrin and does not exit.

One possible explanation is that the catecholate ligand is facilitating oxidation of Am(III) to Am(IV) and promoting the formation of a very stable transferrin complex similar to that of Pu(IV). Catechol has a tremendous ability to stabilize higher oxidation states of cerium and plutonium, as indicated by negative shifts of the (IV)/(III) reduction potential of 1.91 to 2.16 volts for 3,4,3-LICAMS and 3,4,3-LICAMC (Figure 10). However, the Am(IV)/(III) reduction couple is very high and requires

an extraordinary stabilization of Am(IV) to give a complex stable in aqueous solution. Many workers have given estimates for the Am(IV)/(III) reduction potential; they range between + 2.0 to + 2.9 V vs NHE.[75-79] Since the reduction potentials of the quinone/catechol couples are near 0 V in strong base, this sets one limit for the oxidizing power of the Am(IV) complex if excess ligand is present.

Differential pulse voltammetry of Am(3,4,3-LICAMS) and Am(3,4,3-LICAMC) from - 0.4 to + 0.7 V vs SCE at slow scan rates (1.5 mV/second) showed only electrochemistry associated with the ligand. Providing the negative shifts in the (IV)/(III) potential seen for plutonium and cerium are similar for americium, the free metal ion potential for Am(IV)/(III) must be at least + 2.6 V vs NHE. Apparently oxidation of the ligand occurs at a lower potential than oxidation of the Am(III) complex.

Upon lowering the pH a precipitate is formed for both Am(3,4,3-LICAMS) (at pH 10.0) and Am(3,4,3-LICAMC) (at pH 10.4). Results of tracer gel chromatography experiments indicate that 3,4,3-LICAMS forms a complex with Am at pH 7.4 of higher molecular weight than the Pu complex[35] (Figure 16).

One method by which to determine whether or not an Am(III)-catecholate complex is formed is by visible spectroscopy. Aqueous Am(III) has a large, sharp absorbance at 503 nm in acidic media due to a transition assigned as $^7F_0 \rightarrow {}^5L_6$ as well as a broad band at 812 nm due to a $^7F_0 \rightarrow {}^7F_6$ transition.[80] Upon complexation of Am(III) by various ligands these bands are known to shift and change in intensity. Figures 17 and 18 illustrate the spectral changes observed in the 503 nm band upon complexation by 3,4,3-LICAMS and 3,4,3-LICAMC. The spectrum

of free Am(III) is of a diluted sample of stock Am(III), included for comparison (in HCl, pH 2). The sloping baseline in the Am-tetracatecholate spectra is due to partial oxidation of the ligand. Although the ligand solutions were prepared under argon and rigorously degassed, the transfer procedure into the cuvette causes a limited exposure to air and consequent partial oxidation of the free ligand. Nonetheless, the shift in the 503 nm band observed is conclusive evidence of complexation of Am(III) by 3,4,3-LICAMS and 3,4,3-LICAMC.

It is noteworthy that the spectrum of Am(III) with 3,4,3-LICAMS and with 3,4,3-LICAMC are significantly different. This is indicative of a different type of bonding of the two tetracatecholates with Am(III). Although it is impossible to determine the identity of the coordinating groups, the 3,4,3-LICAMC ligand does possess carboxylate groups capable of coordinating Am(III). Polycarboxylatoamines are known to bind Am(III) with high affinity.[81]

The results of these experiments indicate that americium is probably not present as Am(IV) <u>in vivo</u> Indeed, it proves that 3,4,3-LICAMS and 3,4,3-LICAMC form complexes with Am(III) of undetermined stoichiometry and stability. The solution chemistry of Eu(III), a homolog of Am(III), with 3,4,3-LICAMS and several monomeric catechols [catechol, Tiron and N,N-dimethyl-2,3-dihydroxy-5-sulfobenzamide (DMBS), which is structurally the same as the CAM moieties of 3,4,3-LICAMS] have been examined in order to model the behavior of Am(III).[41] Below pH 9 catechol and Tiron form 1:1 Eu complexes, while DMBS forms a 3:2 (ligand:metal) complex, regardless of ligand excess. Surprisingly, 3,4,3-LICAMS with its four pairs of phenolic groups also forms only a 3:2 catechoyl arm:Eu complex, in which three OH groups per ligand were deprotonated for each metal ion bound.

A Job's plot[82] of the Eu(III)-DMBS complex is shown in Figure 19, where the molar ratios of ligand to Eu(III) were varied over a wide range while maintaining [Eu(III)] + [ligand] constant. The maxima in the plot gives the 3:2 stoichiometry of the Eu(III)-DMBS complex in solution.

The Eu-catechol complex is very weak, and above pH 7 excess catechol was not able to prevent precipitation of $Eu(cat)OH \cdot 4H_2O$. The Eu complexes with the sulfonated catecholates are more stable, and above pH 7 formation of insoluble hydrolysis products was prevented. For Eu-Tiron, log K_f is 13.2, about two log units greater than for catechol, in accord with its greater acidity.

Titrations of Eu(III) with 3,4,3-LICAMS indicate that a complex is formed whereby 1.5 catechol arms bind Eu(III) at pH 5.5. At higher pH values some hydroxide also appears to be involved in coordination and equilibrium is achieved only slowly. It seems likely that the Am(III) (3,4,3-LICAMS) complex is similar.

Recently it has been established that monocatecholates can act as the necessary synergistic anion required in the binding of Fe(III) to transferrin, although the catecholates are not thermodynamically favored over the natural synergistic anion carbonate.[83] This does however establish the existence of ternary catechol-Fe(III)-transferrin complexes. One possible explanation for the unusual plasma clearance curves of the Am(3,4,3-LICAMS and Am(3,4,3-LICAMC) is the existence of a ternary complex of tetracatecholate-Am-transferrin.

Summary

The synthesis of a series of tetracatecholate ligands designed to be specific for Pu(IV) and other actinide(IV) ions has been achieved.

Although these compounds are very effective as *in vivo* plutonium removal agents, potentiometric and voltammetric data indicate that at neutral pH full complexation of the Pu(IV) ion by all four catecholate groups does not occur. This implies more acidic chelating groups must be incorporated in the next cycle of ligand design, synthesis and evaluation for chelating agents specific for Pu(IV).

Spectroscopic results indicate that the tetracatecholates, 3,4,3-LICAMS and 3,4,3-LICAMC, complex Am(III). The Am(IV)/(III)-catecholate couple (where catecholate = 3,4,3-LICAMS or 3,4,3-LICAMC) is not observed, but may not be observable due to the large currents associated with ligand oxidation. However, within the potential range where ligand oxidation does not occur, these experiments indicate that the reduction potential of free Am(IV)/(III) is probably $\geq$ + 2.6 V vs NHE or higher. Proof of the complexation of americium in the trivalent oxidation state by 3,4,3-LICAMS and 3,4,3-LICAMC eliminates the possibility of tetracatecholates stabilizing Am(IV) *in vivo*.

Acknowledgments

We acknowledge the contribution to this paper by Dr. Zhu, Daohong and we thank her for allowing the citation of some of her unpublished work. We thank our other co-workers, past and present, whose contributions are cited in the references. This work was supported by the Director, Office of Energy Research, Office of Basic Energy Sciences, Chemical Sciences Division of the U.S. Department of Energy under Contract Number DE-AC03-76SF00098.

References

1. Blomeka, J. O.; Nichols, J. P.; McLain, W. C. Physics Today, August 1973, 26, 36-42.
2. Kube, A. S.; Rose, D. J. Science, 1973, 182, 1205-11.
3. Bienvenu, P.; Nofre, C.; Cier, A. C. R. Acad. Sci., 1963, 256, 1043-4.
4. Stannard, J. N. "The Health Effects of Plutonium and Radium"; Jee, W. S. S., Ed.; J. W. Press: Salt Lake City, 1976; pp 362-72.
5. Durbin, P. W. "Handbook of Experimental Pharamacology, Vol. 36: Uranium, Plutonium, Transplutonic Elements"; Hodge, H. C.; Stannard, J. N.; Hursh, J. B., Eds.; Springer-Vergag: New York, 1973; pp 739-896.
6. Denham, D. H. Health Physics, 1969, 16, 475-87.
7. Bair, J. C.; Thompson, R. C. Science, 1974, 183, 715-22.
8. Jones, M. M.; Pratt, T. H. J. Chem. Ed., 1976, 53, 342-7.
9. Durbin, P. W. Health Physics, 1975, 29, 495-510.
10. International Commission on Radiological Protection, Publication 19: "The Metabolism of Compounds of Plutonium and Other Actinides"; Pergamon Press: New York, 1972.
11. Rundo, J.; Starzyk, P. M.; Sedlet, J.; Larsen, R. P.; Oldham, R. D.; Robinson, J. J. "Diagnosis and Treatment of Incorporated Radionuclides"; International Atomic Energy Agency: Vienna, 1976; pp 15-23.
12. Vaughan, J.; Bleany, B.; Taylor, D. M. "Handbook of Experimental Pharmacology, Vol. 36: Uranium, Plutonium, Transplutonic Elements"; Hodge, H. C.; Stannard, J. N.; Hursh, J. B., Eds.; Springer-Verlag: New York, 1973; pp 349-502

13. Catsch, A. "Diagnosis and Treatment of Incorporated Radionuclides"; International Atomic Energy Agency: Vienna, 1976; pp 295-305.

14. Smith, V. H. Health Physics, 1972, 22, 765-78.

15. Catsch, A.; Harmuth-Hoene, A-E. Biochemical Pharmacology, 1975, 24, 1557-62.

16. Pachauri, O. P.; Tandon, J. P. J. Inorg. Nucl. Chem., 1975, 37, 2321-3.

17. Pachauri, O. P.; Tandon, J. P. Indian J. Chem., 1977, 15A, 57-8.

18. Pachauri, O. P.; Tandon, J. P. J. Gen. Chem. USSR (Engl. Transl.), 1977, 47, 398-401; Zh. Obshch. Khim., 1977, 47, 433-6.

19. Carey, G. H.; Martell, A. E. J. Am. Chem. Soc., 1968, 90, 32-8.

20. Bogucki, R. F.; Martell, A. E. J. Am. Chem. Soc., 1958, 80, 4170-4.

21. Fried, A. R.; Martell, A. E. J. Am. Chem. Soc., 1971, 93, 4695-700.

22. Grimes, J. H. "Diagnosis and Treatment of Incorporated Radionuclides": International Atomic Energy Agency: Vienna, 1976; pp. 419-60.

23. Cohen, N.; Guilmette, R. Bioinorganic Chem., 1975, 5, 203-10.

24. Seven, M. J. "Metal-Binding in Medicine"; Seven, M. J.; Johnson, L. A., Eds.; J. B. Lippincott: Philadelphia, 1960; pp 95-103.

25. Foreman, H.; Nigrovic, V. "Diagnosis and Treatment of Deposited Radionuclides"; Kornberg, H. A.; Norwood, W. D., Eds.; Excerpta Media Foundation: Amsterdam, 1968; pp 419-23.

26. Planas-Bohne, F.; Lohbreier, J. "Diagnosis and Treatment of Incorporated Radionuclides"; International Atomic Energy Agency; Vienna, 1976; pp 505-15.

27. Taylor, D. M. "Handbook of Experimental Pharmacology, Vol. 36: Uranium, Plutonium, Transplutonic Elements"; Hodge, H. C.; Stannard, J. N.; Hursh, J. B., Eds.; Springer-Verlag: New york, 1973; pp 323-47.

28. Bullman, R. A. Structure and Bonding, 1978, 34, 39-77.

29. Taylor, D. M. Health Physics, 1972, 22, 575-81.

30. Popplewell, D. S. "Diagnosis and Treatment of Incorporated Radionuclides"; International Atomic Energy Agency: Vienna, 1976; pp 25-34.

31. "Microbial Iron Metabolism"; Neilands, J. B., Ed.: Academic Press: New York, 1974.

32. Raymond, K. N. "Advances in Chemistry Series, No. 162: Bioinorganic Chemistry — II"; Raymond, K. N., Ed.; American Chemical Society: Washington, D.C., 1977; pp 33-54.

33. Raymond, K. N.; Carrano, C. J. Acc. Chem. Res., 1979, 12, 183-90.

34. Huheey, J. E. "Inorganic Chemistry: Principles of Structure and Reactivity": Harper and Rowe: New York, 1972; pp 418-22.

35. Lloyd, R. D.; Bruenger, F. W.; Atherton, D. R.; Jones, C. W.; Taylor, G. N.; Stevens, W.; Mays, C. W.; Durbin, P. W.; Jeung, N.; Jones, E. S.; Kappel, M. J.; Raymond, K. N.; Weitl, F. L., manuscipt in preparation.

36. Kappel, M. J.; Nitsche, H.; Raymond, K. N., manuscript in preparation.

37. Shannon, R. D. Acta. Crystallogr., Sect. A, 1976, A32, 751-67.

38. Raymond, K. N.; Smith, W. L. Structure and Bonding (Berlin), 1981, 43, 159-86.

39. Raymond, K. N.; Smith, W. L.; Weitl, F. L.; Durbin, P. W.; Jones, E. S.; Abu-Dari, K.; Sofen, S. R.; Cooper, S. R. Am. Chem. Soc. Symp. Ser., 1981 131, 143-172.

40. Freeman, G. E., work in progress.

41. Zhu, D.; Kappel, M. J.; Raymond, K. N., manuscript in preparation.

42. Casellato, U.; Vidali, M.; Vigato, P. A. Inorg. Chim. Acta, 1976, 18, 77-112.

43. Moseley, P. T. "MTP Int. Rev. Sci.: Inorg. Chem., Ser. Two"; Bagnall, K. W., Ed.; Butterworth: London, 1975; Vol. 7, pp 65-110.

44. Hoard, J. L.; Silverton, J. V. Inorg. Chem., 1963, 2, 235-43.

45. Burdett, J. K.; Hoffmann, R.; Fay, R. C. Inorg. Chem., 1978, 17, 2553-68.

46. Blight, D. G.; Kepert, D. L. Inorg. Chem., 1972, 11, 1556-61.

47. Porai-Koshits, M. A.; Aslanov, L. A. J. Struct. Chem. USSR (Engl. Transl.), 1972, 13, 244-53; Zh. Strukt. Khim., 1972, 13, 266-76.

48. Muetterties, E. L.; Guggenberger, L. J. J. Am. Chem. Soc., 1974, 96, 1748-56.

49. Kepert, D. L. Prog. Inorg. Chem., 1978, 24, 179-249.

50. Sofen, S. R.; Abu-Dari, K.; Freyberg, D. P.; Raymond K. N. J. Am. Chem. Soc., 1978, 100, 7882-7.

51. Sofen, S. R.; Cooper, S. R.; Raymond, K. N. Inorg. Chem., 1979, 18, 1611-16.

52. Latimer, W. M. "Oxidation States of the Elements and Their Potentials in Aqueous Solution", 2nd ed.; Prentice-Hall: Englewood Cliffs, New Jersey, 1962; p 294.

53. Ho, T.-L.; Hall, T. W.; Wong, C. M. Chem. Ind. (London), 1972, 729-30.

54. Raymond, K. N.; Isied, S. S.; Brown, L. D.; Fronczek, F. F.; Nibert, J. H. J. Am. Chem. Soc., 1976, 98, 1767-74.

55. Cooper, S. R.; Koh, T. B.; Raymond, K. N. J. Am. Chem. Soc., 1982, 104, 5092-5102.

56. Magers, K. D.; Smith, C. G.; Sawyer, D. T. Inorg. Chem., 1978, 17, 515-23.

57. Meites, L. "Polarographic Techniques"; Wiley: New York, 1965; p 279.

58. Durbin, P. W.; Jones, E. S.; Raymond, K. N.; Weitl, F. L. Radiat. Res., 1980, 81, 170-87.

59. Weitl, F. L.; Raymond, K. N.; Durbin, P. W. J. Med. Chem., 1981, 24, 203-06.

60. Harris, W. R.; Carrano, C. J.; Cooper, S. R.; Sofen, S. R.; Avdeef, A.; McArdle, J. V.; Raymond, K. N. J. Am. Chem. Soc., 1979, 101, 6097.

61. Borgias, B.; Cooper, S. Koh, Y.; Raymond, K., submitted to J. Am. Chem. Soc.

62. Bard, A. J.; Faulkner, L. R. "Electrochemical Methods"; J. Wiley and Sons: New York, 1980; back cover.

63. Meites, L. "Polarographic Techniques", Second Edition; J. Wiley and Sons: New York, 1965; 203-301.

64. Osteryoung, R. A.; Osteryoung, J. Phil. Trans. R. Lond., 1981, A302, 315-26.

65. Connick, R. E.; McVey, W. H. J. Am. Chem. Soc., 1951, 73, 1798.

66. Weitl, F. L.; Raymond, K. N.; Smith, W. L.; Howard, T. R. J. Am. Chem. Soc., 1978, 100, 1170.

67. Weitl, F. L.; Raymond, K. N. J. Am. Chem. Soc., 1980, 102, 2289.

68. Harris, W. R.; Raymond, K. N.; Weitl, F. L. J. Am. Chem. Soc., 1981, 103, 2667-75.

69. Pecoraro, V.; Scarrow, R.; Kappel, M.; Raymond, K., manuscript in preparation.

70. Kappel, M. J., unpublished results.

71. Keller, H. E.; Osteryoung, R. A. Anal. Chem., 1971, 43, 342-48.

72. Schwarzenbach, G.; Schwarzenbach, K. Helv. Chim. Acta, 1963, 46, 1390.

73. Kappel, M. J.; Raymond, K. N. Inorg. Chem., 1982, 21, 3437.

74. Luk, C. K. Biochemistry, 1971, 10, 2838.

75. Morss, L. R.; Fuger, J. J. Inorg. Nucl. Chem., 1981, 43, 2059.

76. Cunningham, B. B. Ann. Rev. Nucl. Sci., 1964, 14, 323.

77. Nugent, L. J.; Baybarz, R. D.; Burnett, J. L.; Ryan, J. L. J. Phys. Chem., 1973, 77, 1528.

78. Hobart, D. E.; Samhoun, K.; Peterson, J. R. Radiochimica Acta, 1982, 31, 139.

79. Penneman, R. A.; Coleman, J. S.; Keenan, T. K. J. Inorg. Nucl. Chem., 1961, 17, 138.

80. Shiloh, M.; Givon, M.; Marcus, Y. J. Inorg. Nucl. Chem., 1969, 31, 1807.

81. Site, A. D.; Baybarz, R. D. J. Inorg. Nucl. Chem., 1969, 31, 2201.

82. Angelici, R. J. "Synthesis and Technique in Inorganic Chemistry"; W. B. Saunders Co.: Philadelphia, 1969; pp 99-103.

83. Loomis, L., personal communication.

Figure Captions

Figure 1. A tabulation of some of the chemical and biological similarities of Pu(IV) and Fe(III).

Figure 2. The siderophores enterobactin and desferrioxamine B (DFO).

Figure 3. Eight-coordinate polyhedra. The principal axes are vertical. Edge labels are taken from Refs. 44 and 47.

Figure 4. The $[M(O_2C_6H_4)_4]^{n-}$ anion (n = 4 when M = Hf, Ce, Th and U; n = 5 when M = Gd) viewed along the mirror plane with the $\bar{4}$ axis vertical.

Figure 5. A schematic structure of a Pu(IV)-tetracatechoylamide complex.

Figure 6. Structures of 3,4,3-LICAMS and 3,4,3-LICAMC.

Figure 7. The $[Gd(O_2C_6H_4)_3]_2^{6-}$ anion.

Figure 8. Plot of the dependence of $E_{1/2}$ on total catechol concentration (L_T = 12.4 to 1000.0 mM) for the Ce(IV)/Ce(III) couple.

Figure 9. Plot of the dependence of $E_{1/2}$ on total catechol concentration (L_T = 9.0 to 32.0 mM) for the Pu(IV)/Pu(III) couple.

Figure 10. A tabulation of the redox potential shifts for the IV/III couple of Pu and Ce for several catechol ligands.

Figure 11. Differential pulse voltammograms of Pu(3,4,3-LICAMS) as a function of pH (pH 10.59, 10.12, 9.90, 9.68, 9.36, 8.79, 7.39, 6.85).

Figure 12. A plot of the variation of $E_{1/2}$ with pH for Pu(3,4,3-LICAMS).

Figure 13. Plots of the variation of peak current with pH for Pu(3,4,3-LICAMS).

Figure 14. Summary of the Pu polycatecholate equilibria as determined by electrochemistry. The species related by redox or equilibria reactions are shown.

Figure 15. ^{241}Am in plasma of young adult beagles injected with 30 μmol/kg of ligand 30 minutes after nuclide administration (first 3 hours).

Figure 16. Elution profiles on Sephadex G-25 gel of Pu and Am in a 3,4,3-LICAMS solution.

Figure 17. Visible spectra of free Am(III) (0.20 mM, pH 2), Am(3,4,3-LICAMS (0.12 mM, pH 13), Am(3,4,3-LICAMC) (0.12 mM, pH 13).

Figure 18. A summary of Am(III) spectra which shows the effect of catechol complexation compared to the free aquo complex.

Figure 19. A Job's plot (absorbance as a function of ligand/metal mole ratio) of Eu(III) and N,N-dimethyl-2,3-dihydroxy-5-sulfobenzamide (DMBS).

Similarities of Pu^{4+} and Fe^{3+}

$$\frac{\text{Charge}}{\text{Ionic radius}} \qquad Pu^{4+} \ \frac{4}{.96} = 4.2 \qquad\qquad Fe^{3+} \ \frac{3}{.65} = 4.6$$

$$Fe(OH_3) \rightleftharpoons Fe^{3+} + 3OH^- \qquad K \approx 10^{-38}$$

$$Fe^{3+} + H_2O \rightleftharpoons Fe(OH)^{2+} + H^+ \qquad K = 0.0009$$

$$Pu(OH)_4 \rightleftharpoons Pu^{4+} + 4OH^- \qquad K \approx 10^{-55}$$

$$Pu^{4+} + H_2O \rightleftharpoons Pu(OH)^{3+} + H^+ \qquad K = 0.031 \quad (\text{in } HClO_4)$$

Pu^{4+} transported in blood plasma of mammals as a complex of transferrin (the normal transport agent of Fe^{3+}). The Pu^{4+} binds at same site as Fe^{3+}.

XBL 772-7583

Figure 1.

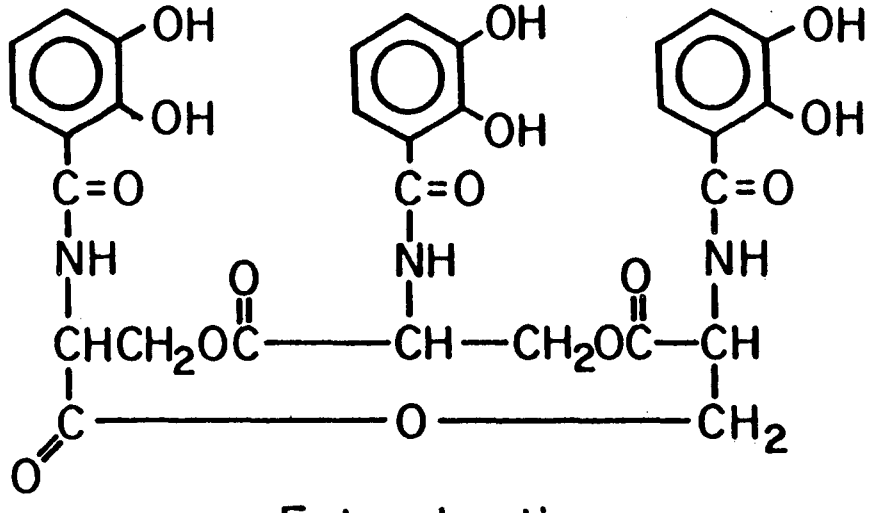

Enterobactin

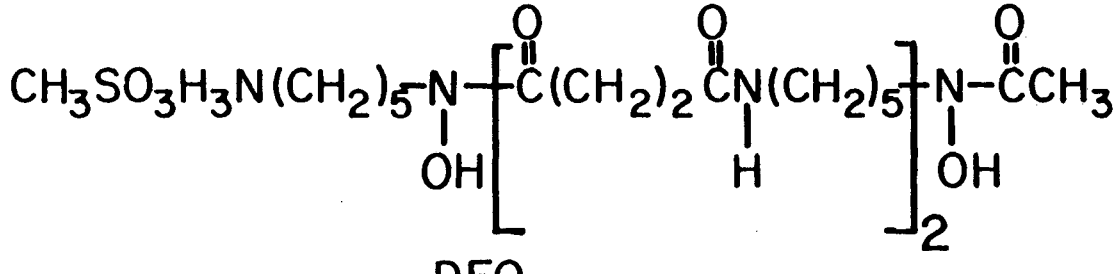

DFO

XBL794-3346

Figure 2.

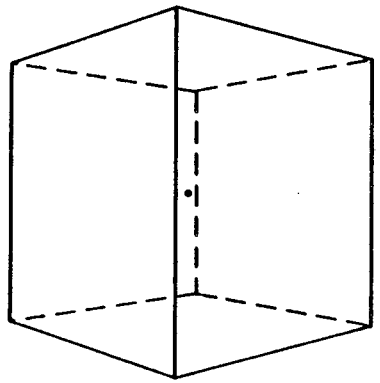

Cube
O_h

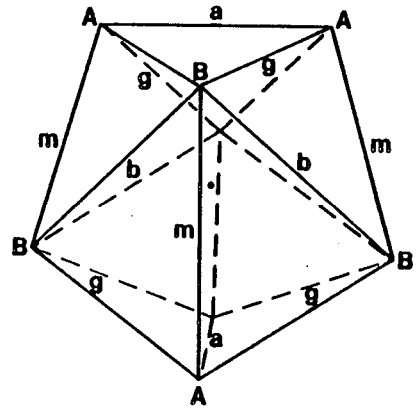

Dodecahedron
D_{2d}

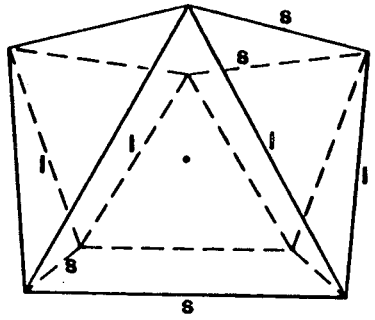

Square Antiprism
D_{4d}

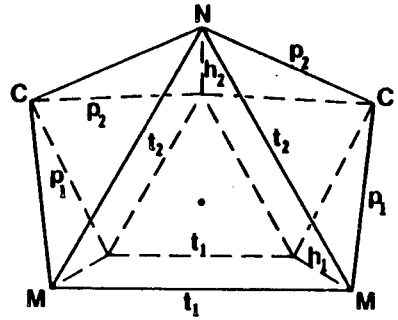

Bicapped Trigonal Prism
C_{2v}

XBL 799-11289

Figure 3

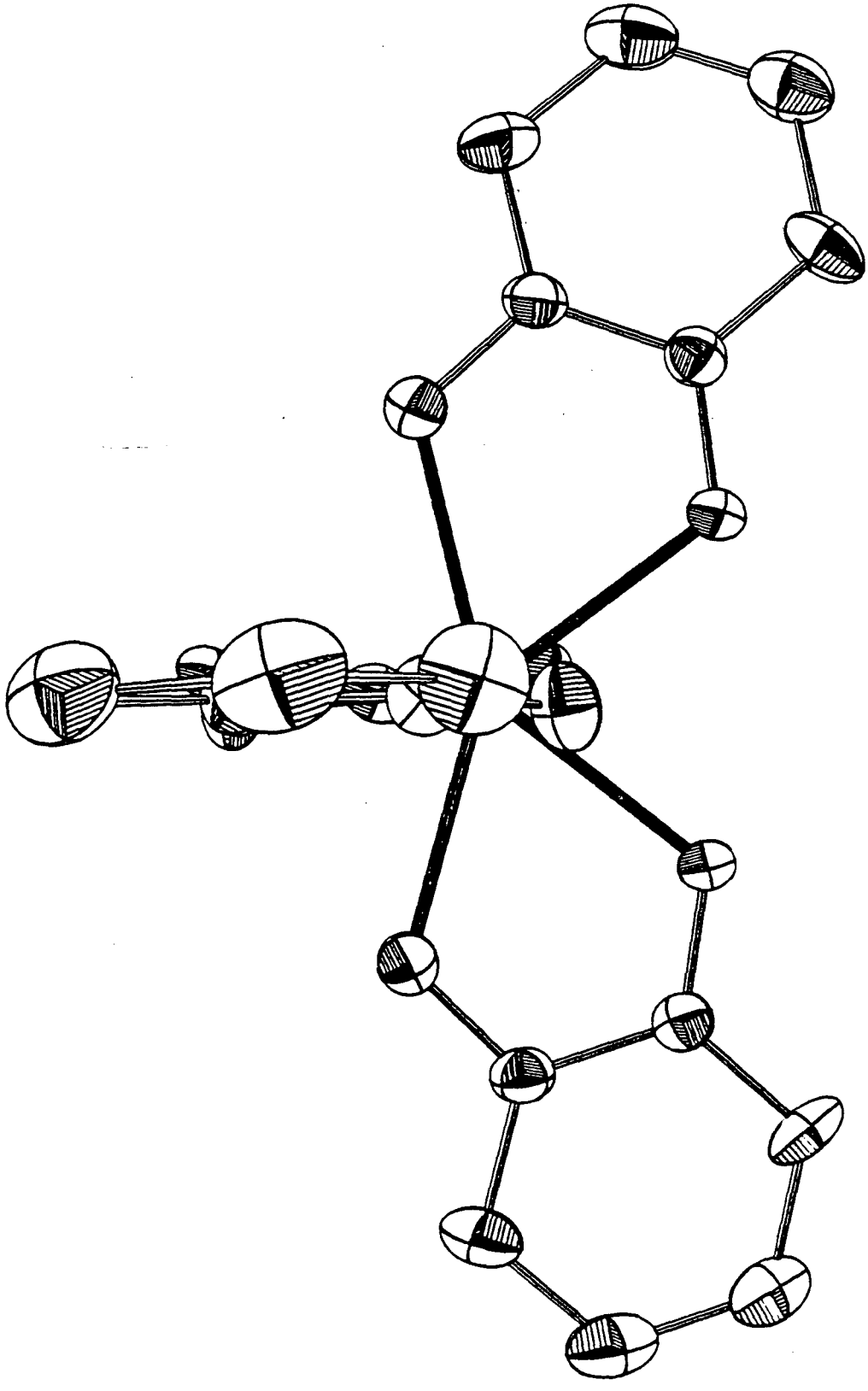

XBL 781-6965

Figure 4.

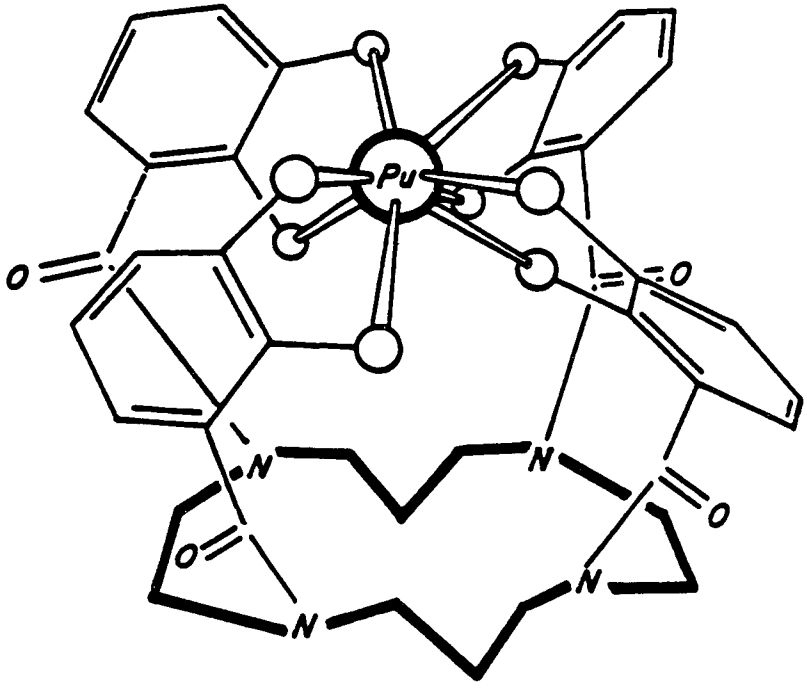

XBL 772-7549

Figure 5.

CATECHOYLAMIDE LIGANDS

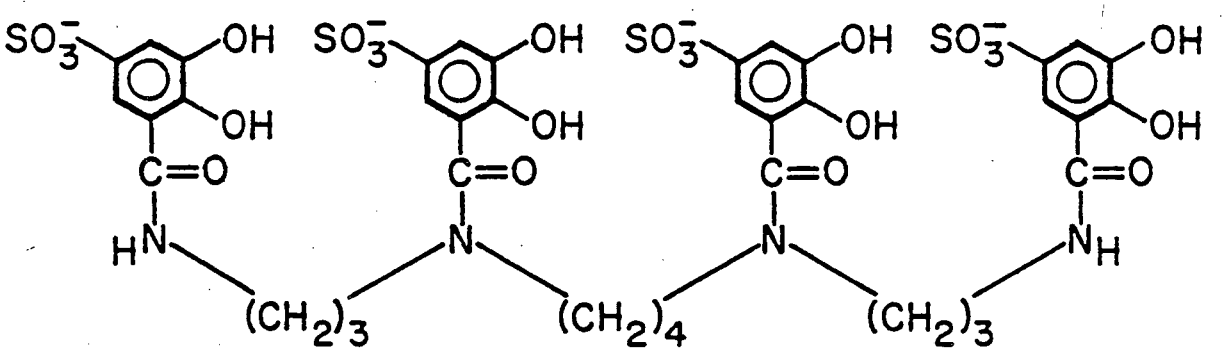

3,4,3-LICAMS

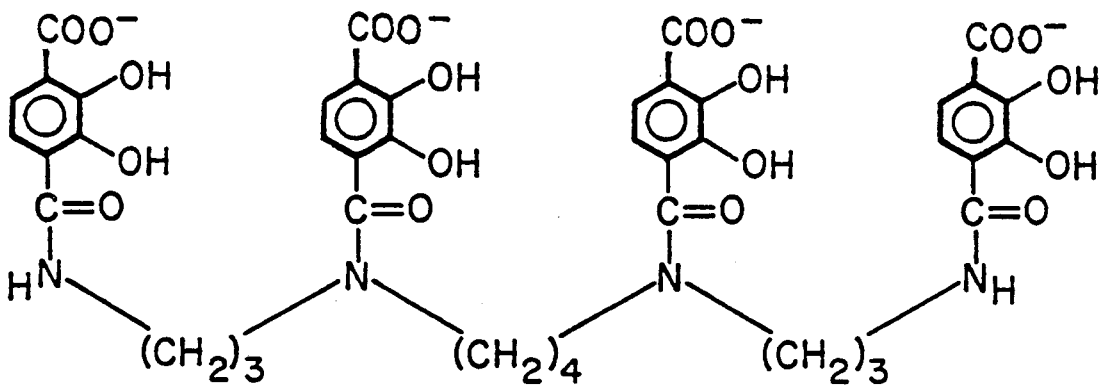

3,4,3-LICAMC

XBL 833-8708

Figure 6.

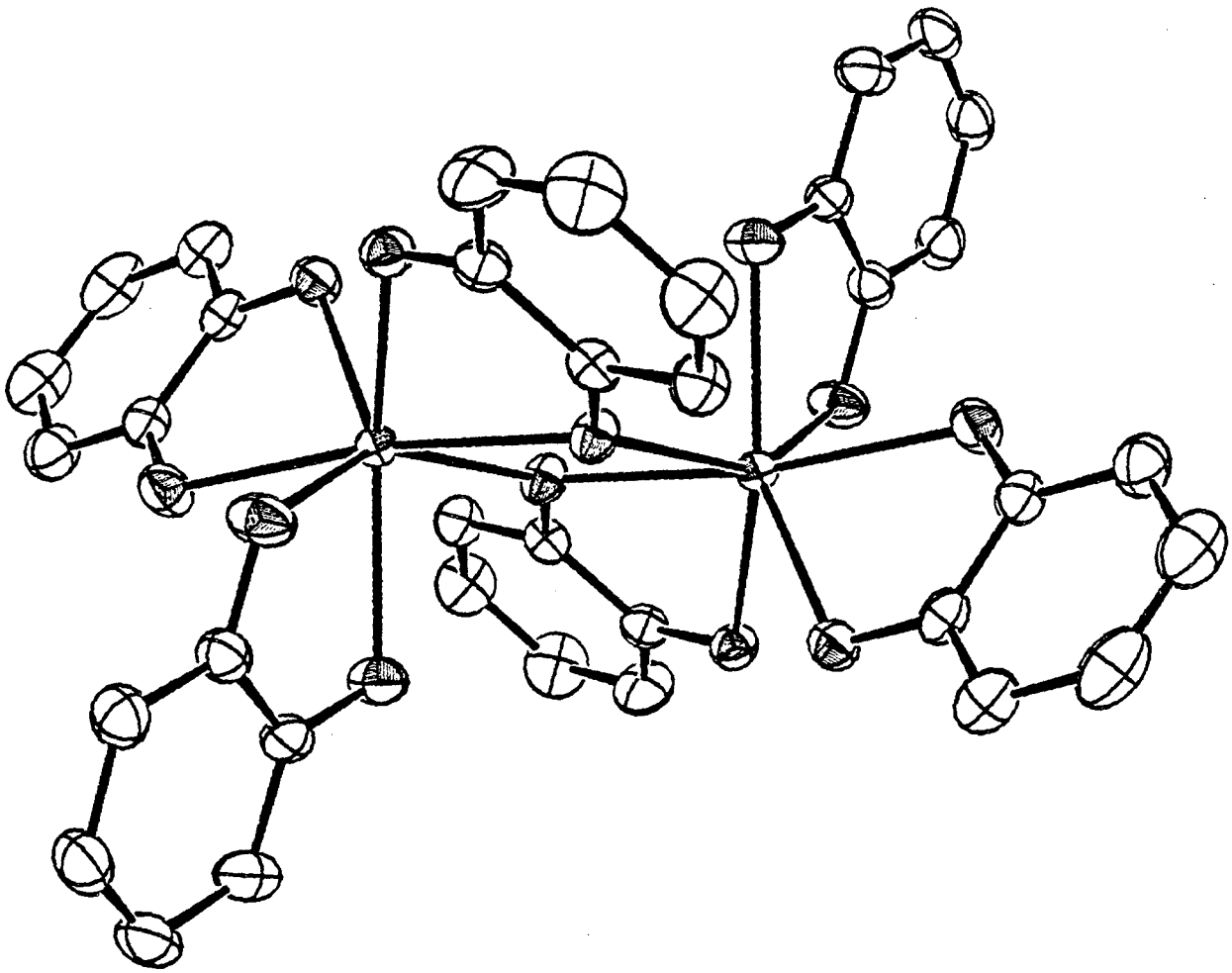

XBL 838-504

Figure 7.

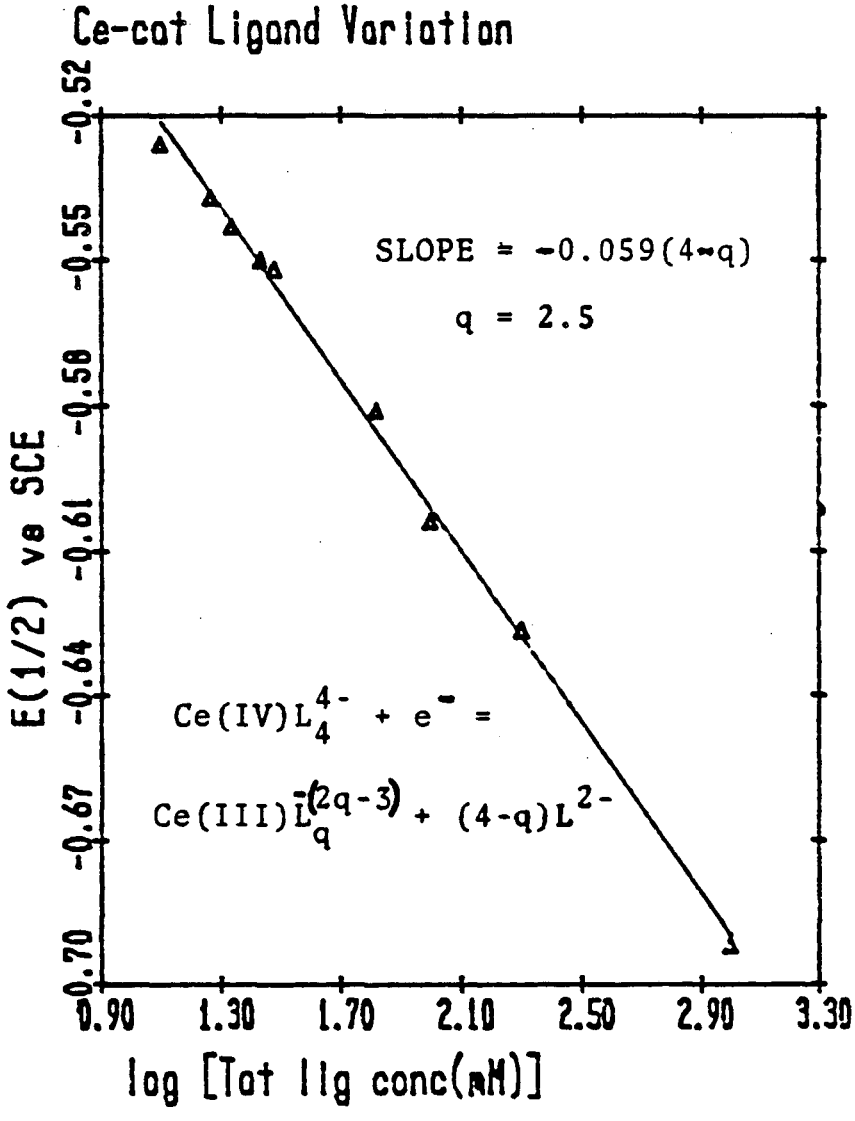

XBL 837-10656

Figure 8.

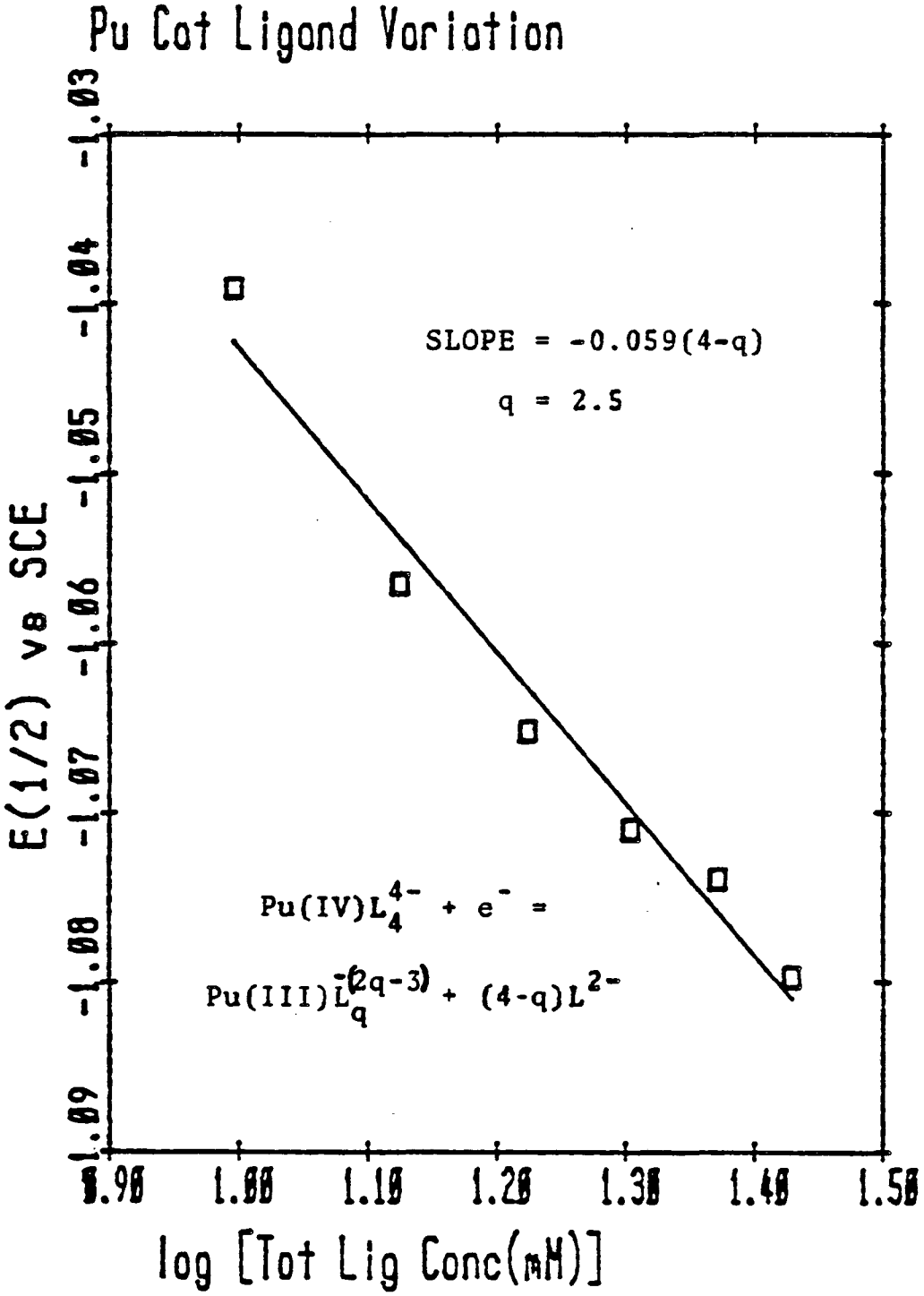

XBL 837-10655

Figure 9.

Potential Shifts of Catecholate-bound Pu and Ce

Ligand	Shift of Ce(IV)/Ce(III)[a] (Volts)	Shift of Pu(IV)/Pu(III)[b] (Volts)
Catechol	-2.00	-1.82
Tiron[c]	-1.97	-2.07
3,4,3-LICAMS	-2.11	-1.91
3,4,3-LICAMC	-2.16	-2.03

Potential in 1 M $HClO_4$ vs. NHE:

a. $Ce(IV) + e^- = Ce(III)$ + 1.7 Volts

b. $Pu(IV) + e^- = Pu(III)$ + 0.98 Volts

c. Irreversible

Figure 10.

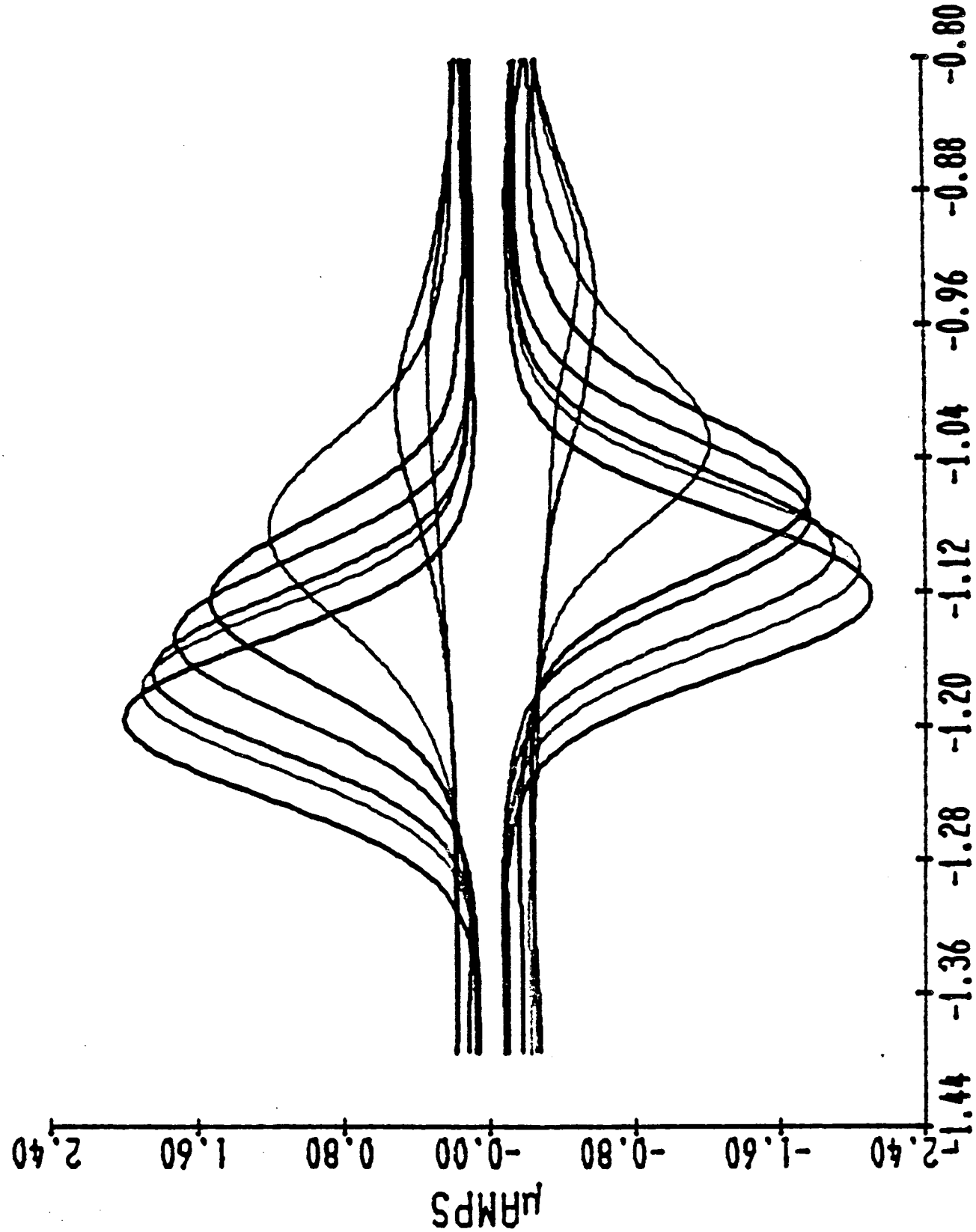
μAMPS
2.40
1.60
0.80
-0.00
-0.80
-1.60
-2.40
-1.44
-1.36
-1.28
-1.20
-1.12
-1.04
-0.96
-0.88
-0.80
VOLTS vs SCE

Figure 11.

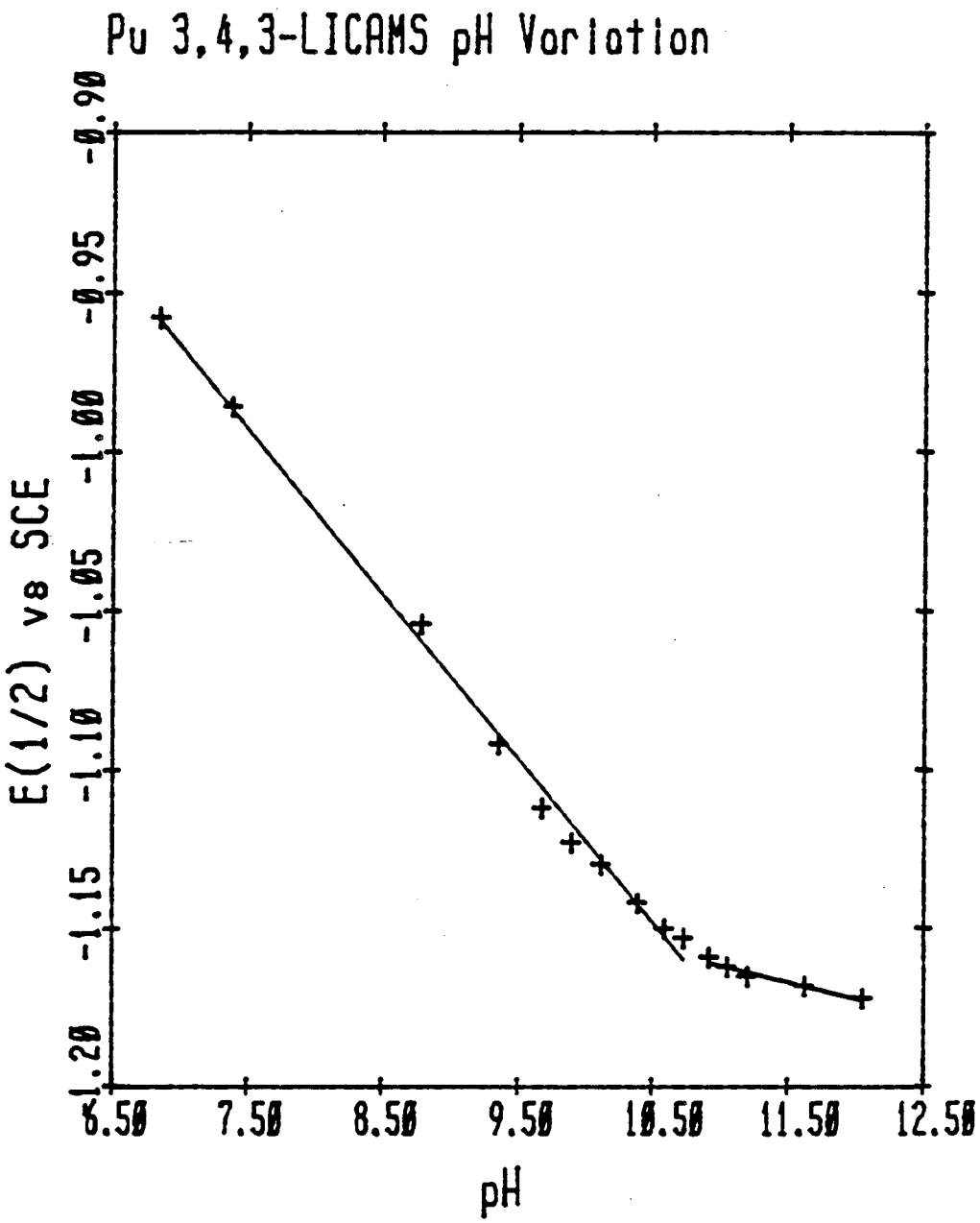

XBL 833-8710

Figure 12.

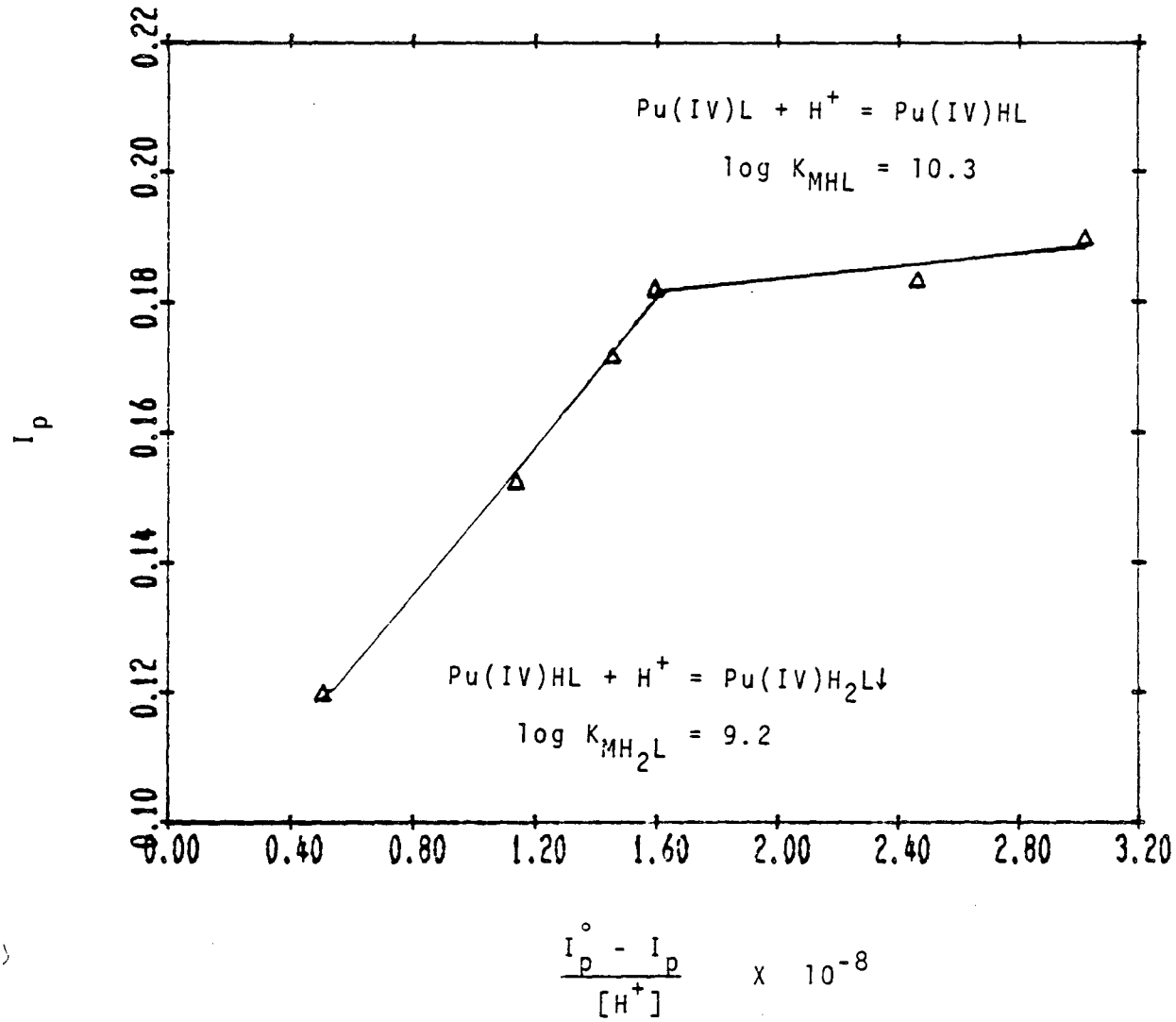
Pu(IV)L + H+ = Pu(IV)HL
log KMHL = 10.3
Pu(IV)HL + H+ = Pu(IV)H2L↓
log KMH2L = 9.2
Ip
0.10
0.12
0.14
0.16
0.18
0.20
0.22
0.00
0.40
0.80
1.20
1.60
2.00
2.40
2.80
3.20
Ip° - Ip / [H+] x 10-8
XBL 833-8712

Figure 13.

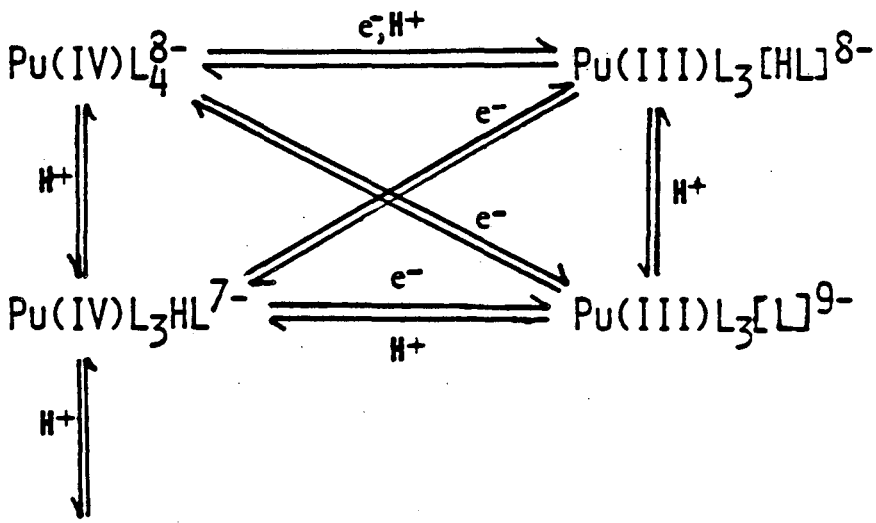

L = BOUND LIGAND ARM [L] = FREE LIGAND ARM

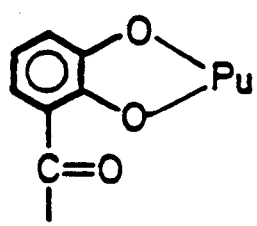

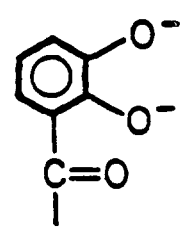

Figure 14.

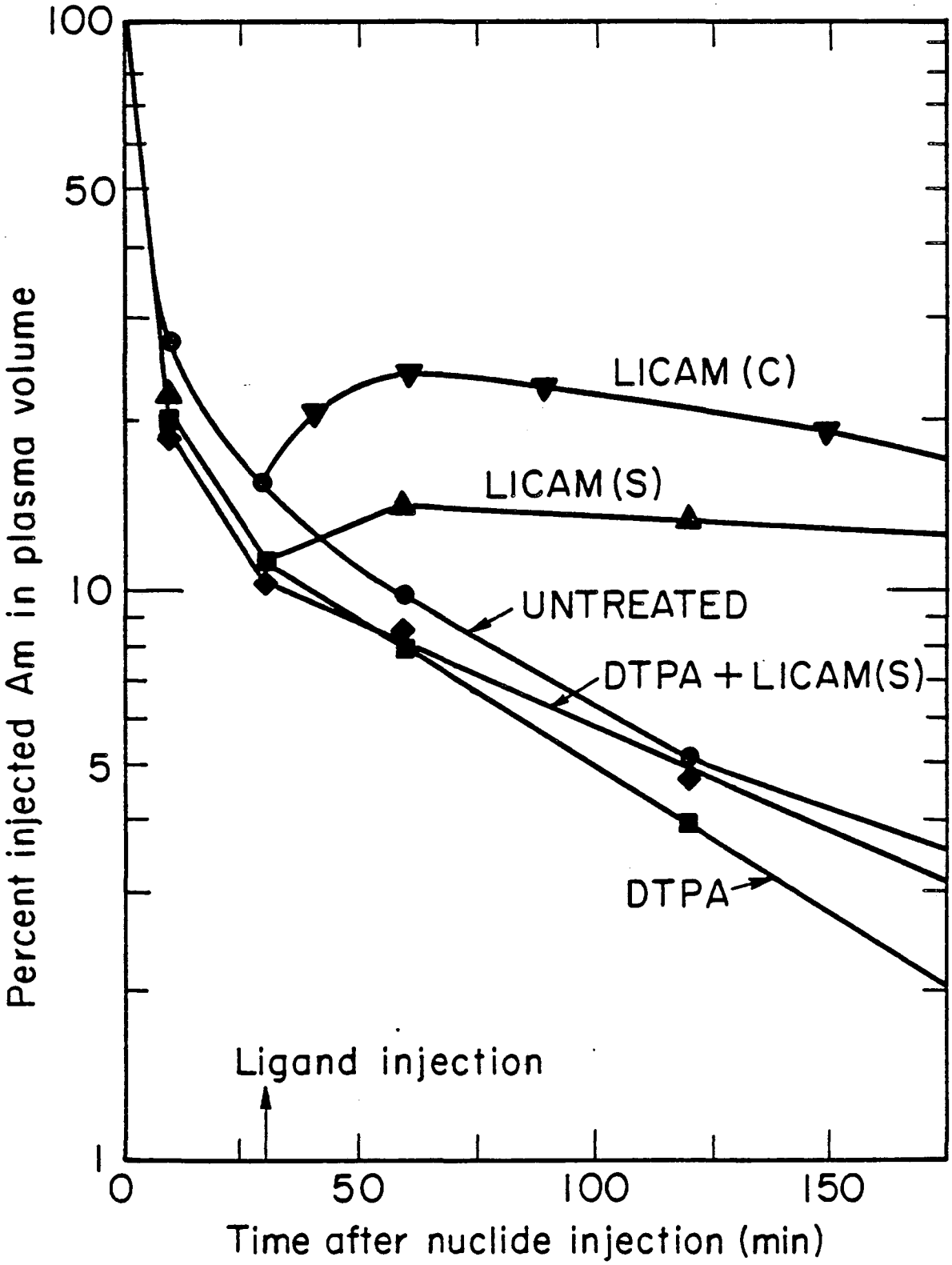
100
50
10
5
1
Percent injected Am in plasma volume
LICAM (C)
LICAM (S)
UNTREATED
DTPA + LICAM(S)
DTPA
Ligand injection
0
50
100
150
Time after nuclide injection (min)
XBL834-3695

Figure 15.

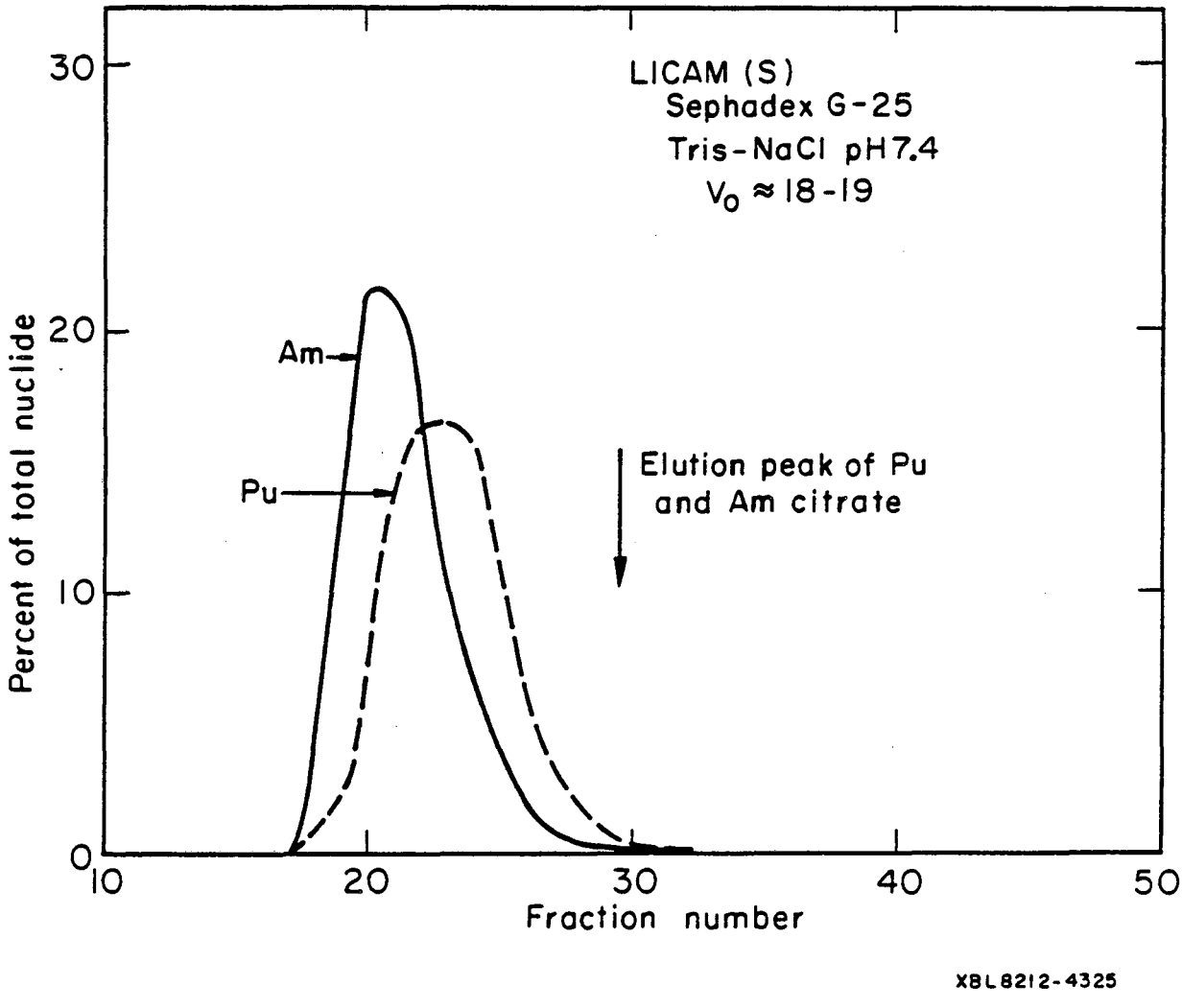
LICAM (S)
Sephadex G-25
Tris-NaCl pH7.4
$V_0 \approx 18-19$
Am
Pu
Elution peak of Pu
and Am citrate
Percent of total nuclide
Fraction number
0
10
20
30
40
50
XBL8212-4325

Figure 16.

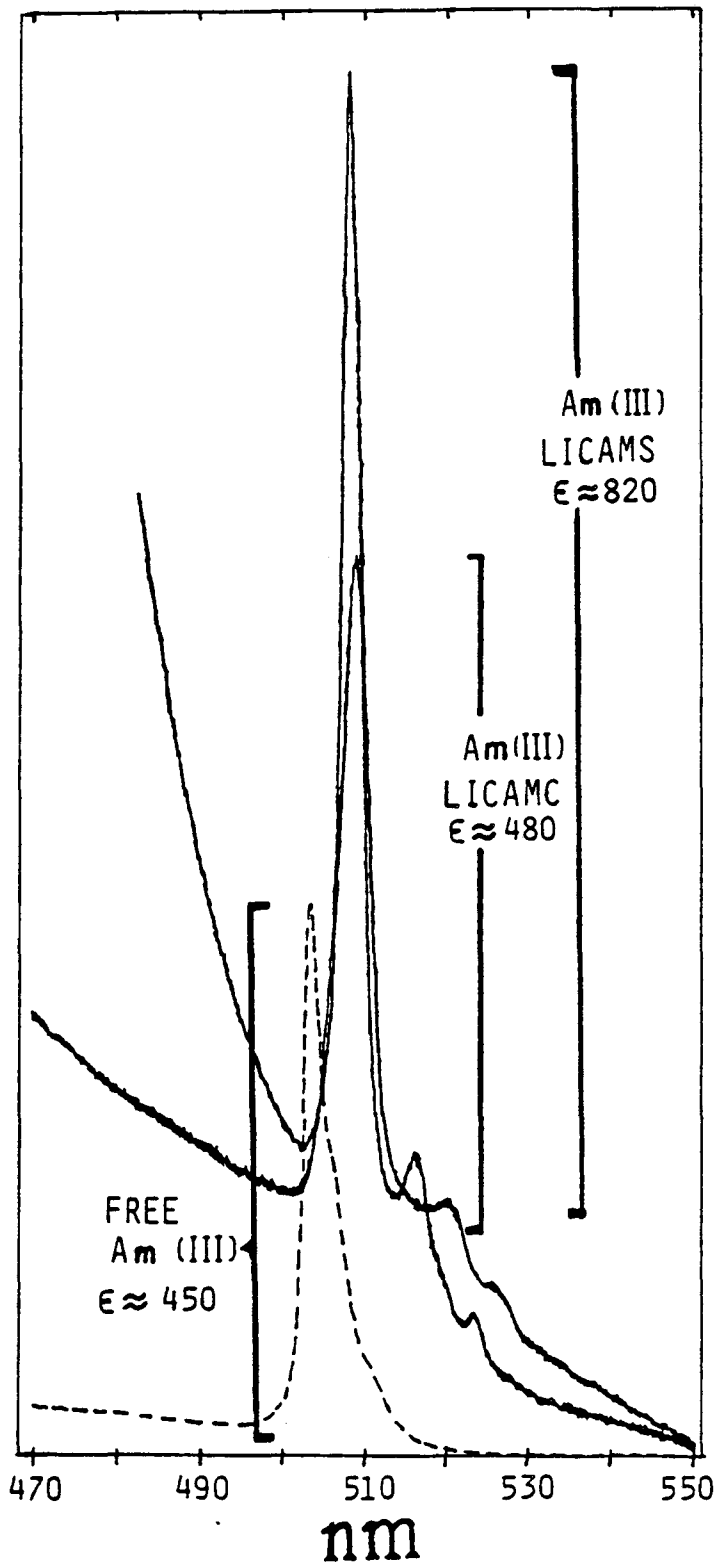
Am (III)
LICAMS
ε≈820
Am(III)
LICAMC
ε≈480
FREE
Am (III)
ε≈ 450
470
490
510
530
550
nm
XBL 837-10657

Figure 17.

Summary of Am(III) Spectra

	Band I[a] nm	Band II[b] nm
Free Am(III)	503(450)	812(77)
Am(III)(3,4,3-LICAMS)	507(822) 516(97) 523(24)	815(80)
Am(III)(3,4,3-LICAMC)	508(482) 520(59) 526(28)	830(126)

[a]Sharp band and satellites. Extinction coefficients in units of M^{-1} cm^{-1} are in parentheses.

[b]Broad band. Extinction coefficients in units of $M^{-1}cm^{-1}$ are in parentheses.

Figure 18.

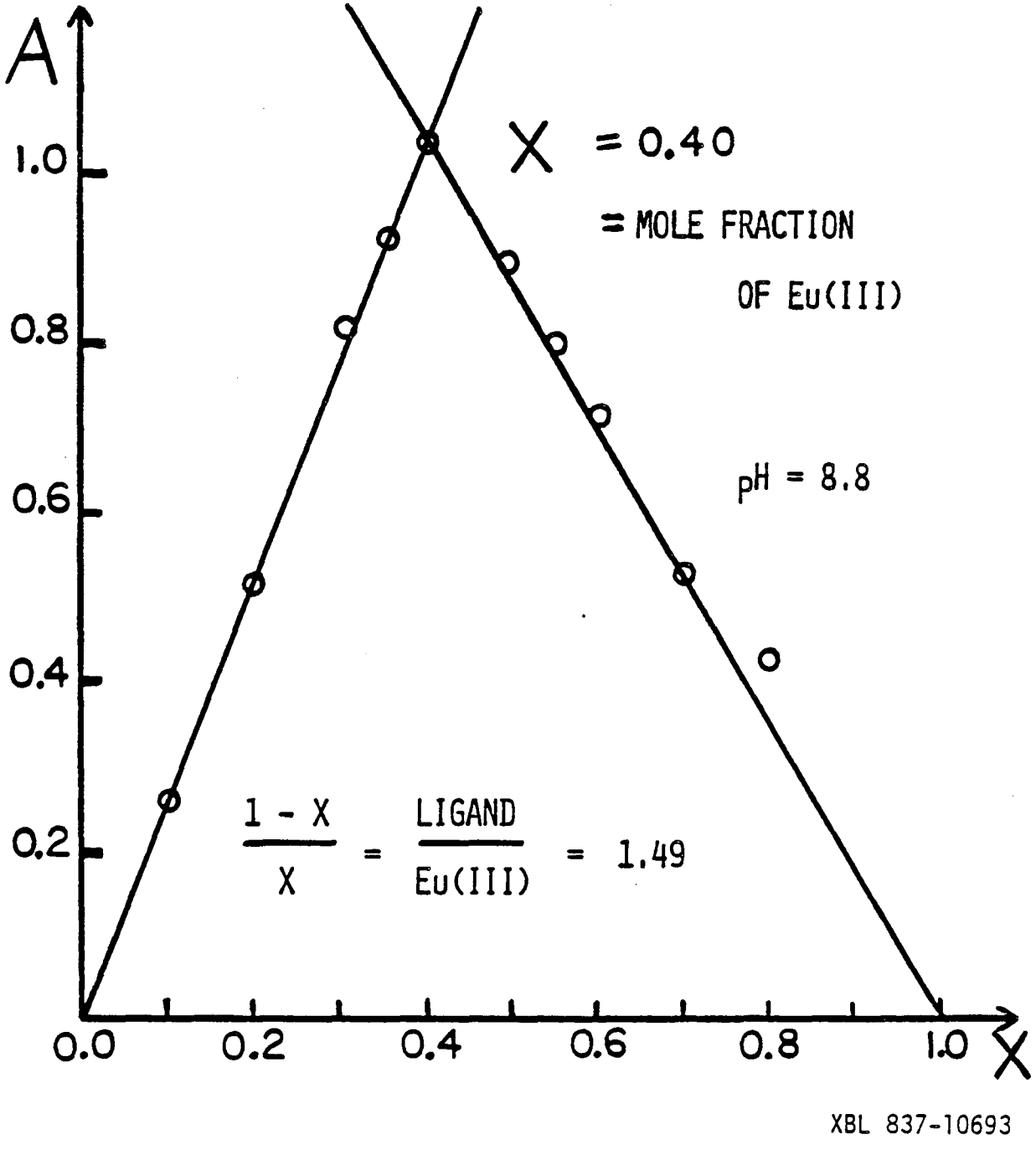
A
1.0
0.8
0.6
0.4
0.2
0.0
0.2
0.4
0.6
0.8
1.0
X
X = 0.40
= MOLE FRACTION
OF Eu(III)
pH = 8.8
1 - X / X = LIGAND / Eu(III) = 1.49
XBL 837-10693

Figure 19.

TECHNICAL INFORMATION DEPARTMENT
LAWRENCE BERKELEY LABORATORY
UNIVERSITY OF CALIFORNIA
BERKELEY, CALIFORNIA 94720